7

δ-Free F_oF_1-ATPase, Nanomachine and Biosensor

Jia-Chang Yue[1], Yao-Gen Shu[2], Pei-Rong Wang[1] and Xu Zhang[1]
[1]*Institute of Biophysics, Chinese Academy of Sciences*
[2]*Institute of Theoretical Physics, Chinese Academy of Sciences*
China

1. Introduction

F_oF_1-ATPase is an exquisite nanomachines self-assembled by eight kinds of subunits, and is ubiquitous in the plasma membrane of bacteria, chloroplasts and mitochondria as well as uses the transmembrane electrochemical potential to synthesize ATP. The holoenzyme is a complex of two opposing rotary motors, F_o and F_1, which are mechanically coupled by a common central stalk ("rotor"), $c_n\epsilon\gamma$, and δb_2 subunits connecting two "stator", $\alpha_3\beta_3$ crown in F_1 and a in F_o. The membrane embedded F_o unit converts the proton motive force (p.m.f.) into mechanical rotation of the "rotor", thereby causing cyclic conformational change of $\alpha_3\beta_3$ crown ("stator") in F_1 and driving ATP synthesis. A striking characteristic of this motor is its reversibility. It may rotate in the reverse direction for ATP hydrolysis and utilize the excess energy to pump protons across the membrane(Ballmoos et al., 2009; Boyer, 1997; Feniouk & Yoshida, 2008; Junge, 2004; Saraste, 1999; Weber & Senior, 2003).
The basic hypothesis, "binding change mechanism"(Boyer et al., 1973), however, had not been confirmed until the direct observation of the rotation of F_1-ATPase at single molecule level in 1997(Noji et al., 1997), although it was partly proven by the eccentric structure of γ subunit in 1994(Abrahams et al., 1994). Single molecule technologies have contributed very much to the motor. For example, fluorescence imaging and spectroscopy revealed the physical rotation of isolated F_1(Adachi et al., 2007; Nishizaka et al., 2004; Noji et al., 1997; Yasuda et al., 1998) and F_o(Düser et al., 2009; Zhang et al., 2005), or F_1F_o holoenzyme(Diez et al., 2004; Kaim et al., 2002; Ueno et al., 2005). Magnetic tweezers also be employed to manipulate the ATP synthesis/hydrolysis in F_1(Itoh et al., 2004; Rondelez et al., 2005), and proton translation in F_o(Liu et al., 2006a). Recently, a membrane scaffold protein has been applied to observe the stepping rotation of proton channels (c_n)(Ishmukhametov et al., 2010).
There are three catalytic sites localized three identical β subunits in F_1 respectively. However, the three sites have different affinities for substrate at any given moment in time during catalysis. On the other hand, with different technologies such as AFM, Electron density, and laser-induced liquid bead ion desorption-MS(LILBID-MS) etc., the number of proton channels have been revealed ranging from 10 to 15 for different species(Jiang et al., 2001; Meier et al., 2007; Mitome et al., 2004; Pogoryelov et al., 2005; Seelert et al., 2000; Stock et al., 1999). Thus, it seems reasonable that three ATP molecules will be generated/consumed in F_1 for every cycle, at the same time $n(10 \sim 15)$ protons will be translated transmembrane in F_o because of the tight coupling between the two motors. That is, the H^+/ATP ratio should be $3/n$.
With the development of gene engineering, all subunits of the motor can be expressed in *E. Coli*. such that the motor can be self-assembled *in vitro* into a nanodevice for different

application(Choi & Montemagno, 2005; Liu et al., 2002; Luo et al., 2005; Martin et al, 2007; Soong et al., 2000). For example, if the δ subunit is removed from the motor, the two stators are structurally uncoupled, thereby the F_1 stator only contact with the common rotor. This is named δ-free F_oF_1 motor. Its stator is the a and b_2 subunits, while the rotor is built by c_n, ϵ, γ and $\alpha_3\beta_3$ subunits. Furthermore, this motor can be embedded in a chromatophore which functions as a battery recharged by illumination. Thus, the motor has been reconstructed into a self-driven nanomachine in which the only power is the transmembrane p.m.f. Here, we briefly review our works on the δ-free F_oF_1 motor including reconstituting, direct observation of its rotation, developing as a biosensor and a activator, and so on. However, we begin with the enzymatics of the holoenzyme to investigate the relation between the rotation speed and substrate/product concentrations, transmembrane p.m.f. and damping coefficient etc. which is of benefit to the quantitative analysis.

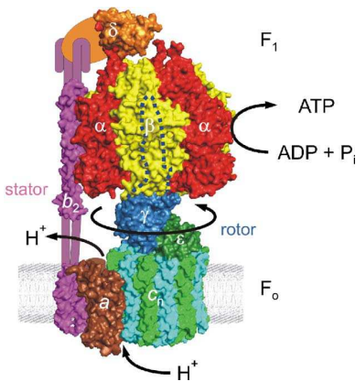

(a) Structure of F_oF_1-ATPase

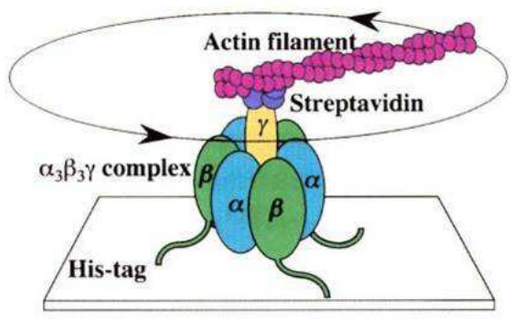

(b) Single-molecule experiment of isolated F_1

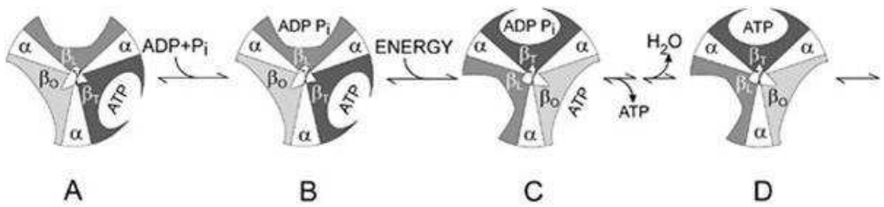

(c) Binding Change Mechanism of ATP synthase

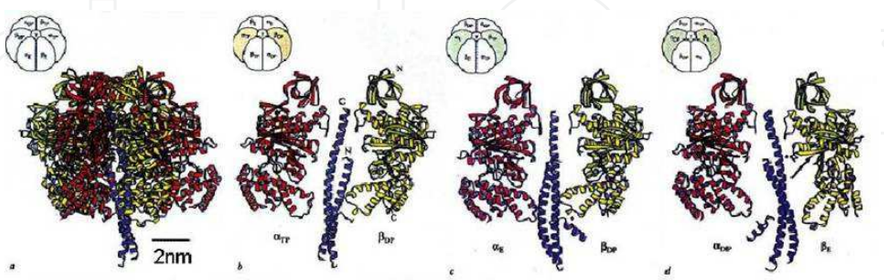

(d) The crystal structure of F_1

Fig. 1. The full-atom structure of the F_oF_1-ATPase(a)(Weber, 2006) and three main breakthroughs including direct observation of rotation of F_1(b)(Noji et al., 1997), basic hypothesis of "binding change mechanism" for ATP synthase(c)(Boyer, 1997) and crystal structure proving of the eccentric rotation of γ subunit(d)(Abrahams et al., 1994).

2. Enzymatics of the holoenzyme

From the viewpoint of enzymatics, conventional theory generally concerned with irreversible reaction on a single substrate which can be described by the Michaelis-Menten kinetics. But ATP can be reversibly synthesized and hydrolyzed in F_oF_1-ATPase, and the reaction involves several substrates/products. In particular, ATP hydrolysis does spontaneously occur in F_1, whereas the thermodynamically unfavorable reaction, ATP synthesis, has to be driven by harnessing the transmembrane proton flow in F_o. If it functions as a synthase, the two substrates, ADP and P_i, are recombined into one product, ATP. Though it is well established that the mechanical process, chemical reactions in F_1 and transmembrane proton transport in F_o are tightly coupled, that is, three ATP molecules will be generated in F_1 for every cycle with n protons transmembrane translation in F_o, the fundamental relation between the rotation speed and substrate/product concentrations, transmembrane p.m.f. and damping coefficient is still challenging.

2.1 Systematic kinetics of the holoenzyme

A few of theoretical approaches have been proposed aiming for a better understanding of the operating mechanism of this reversible motor. Some work focused on the hydrolysis or synthesis of F_1. For example, Oster *et al.* constructed a 4^3 states model for the couplings among three catalytic sites and provided a physical view of the dynamics(Sun et al., 2004; Wang & Oster, 1998; Xing et al., 2005). However, the model is too sophisticated to be investigated analytically. Some other models studied the mechanism of torque generation of F_o with a turbine or all-atom model(Aksimentiev et al., 2004; Elston et al., 1998; Oster et al., 2000). On the other hand, the kinetics of this motor has been investigated by Pänke *et al.* with simulations or storage of elastic energy model(Pänke & Rumberg, 1996; 1999). Here, we focus on analytical investigation of the systematic kinetics of the holoenzyme. Furthermore, presumably analytical results could allow for a deeper insight for the working principles of the motor.

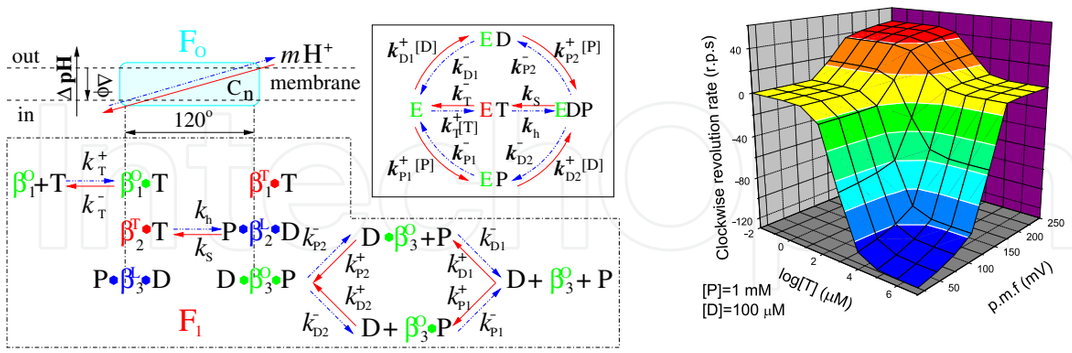

(a) Tri-site filled with random order binding model. (b) Speed versus ATP concentration and p.m.f.

Fig. 2. (a) Tri-site filled with random order binding model. Synthesis pathway runs from right to left (red solid), whereas hydrolysis one runs from left to right (blue dash dots). (b) Rotational speed of motor versus ATP concentration and p.m.f. Red or blue means that motor works in synthesis or hydrolysis respectively, and yellow represents that motor is near equilibrium(Shu & Lai, 2008).

It is well established that the mechanical process in F_o and the chemical reactions in F_1 are tightly coupled. Therefore, it is possible to construct a theory which can systematically describe the whole machine. Here, we propose a tri-site filled with random order of ADP and P_i binding model (shown in Fig.2(a)). The kinetics of this reversible reaction may be described by the equations governing the probabilities(denoted by P_E, P_{ET}, P_{EDP}, P_{ED}, and P_{EP}) of these five states:

$$\left.\begin{aligned}
\dot{P}_E &= k_T^- P_{ET} + k_{D1}^- P_{ED} + k_{P1}^- P_{EP} - (k_{D1}^+[D] + k_{P1}^+[P] + k_T^+[T])P_E \\
\dot{P}_{ET} &= k_T^+[T]P_E + k_s P_{EDP} - (k_T^- + k_h)P_{ET} \\
\dot{P}_{EDP} &= k_h P_{ET} + k_{P2}^+[P]P_{ED} + k_{D2}^+[D]P_{EP} - (k_{D2}^- + k_{P2}^- + k_s)P_{EDP} \\
\dot{P}_{ED} &= k_{P2}^- P_{EDP} + k_{D1}^+[D]P_E - (k_{D1}^- + k_{P2}^+[P])P_{ED} \\
P_{EP} &= 1 - (P_E + P_{ET} + P_{EDP} + P_{ED})
\end{aligned}\right\}, \tag{1}$$

where the square bracket [ ] denotes the concentration, T, D and P represent ATP, ADP and P_i respectively, and $k^+(k^-)$ is the binding(unbinding) constant. The steady-state reaction rate has been derived to be of second degree in ADP and P_i concentrations, and cannot be treated in terms of a Michaelis-Menten form. However, if the bindings and unbindings of ADP and P_i are completely independent and there is no mutual interaction, i.e. $k_{D1}^{\pm} = k_{D2}^{\pm} \equiv k_D^{\pm}$ and $k_{P1}^{\pm} = k_{P2}^{\pm} \equiv k_P^{\pm}$, it can be put into an apparent Michaelis-Menten equation. In addition, clamped ΔpH experiment(Kothen et al., 1995) has shown that binding and unbinding of a substrate (at cosubstrate saturation) are rapid processes as compared to the synthesis/hydrolysis step (mechanical rotation), which means that $k_{s/h} \ll k_L \equiv k_P^+[P] + k_D^+[D] + k_P^- + k_D^-$. Within the framework of steady-state conditions, the clockwise revolution rate of the motor at steady state is given by $\frac{1}{3}(k_s P_{EDP} - k_h P_{ET})$ and can be computed to be

$$r_c = \frac{\frac{1}{3} v_M^s v_M^h \left\{ [D][P] - \frac{[T]}{K_e} \right\}}{(K_M^P[D] + K_M^D[P] + [D][P])\, v_M^h + \frac{K_M^T + \sigma[T]}{K_e} v_M^s}. \tag{2}$$

The definition and meaning of various quantities in the above equation are given below: v_M^s and v_M^h are the saturated rates of synthesis and hydrolysis and are given by

$$v_M^s \equiv \frac{v_{max}^s k_s}{k_s + k_h + v_{max}^s (1 - k_s/k_L)} \approx \frac{v_{max}^s k_s}{k_s + v_{max}^s + k_h}, \tag{3}$$

$$v_M^h \equiv \frac{v_{max}^h k_h}{k_h + v_{max}^h [1 - (k_h - k_s)/k_L]} \approx \frac{v_{max}^h k_h}{k_h + v_{max}^h} \tag{4}$$

respectively, where the maximum rates are $v_{max}^s \equiv k_T^-$ and $v_{max}^h \equiv k_P^- k_D^- / (k_P^- + k_D^-)$.
The corresponding Michaelis constants are given by

$$K_M^T \equiv v_M^h \left[\frac{1}{k_T^-} + \frac{1}{k_h} \left(1 + \frac{k_s}{k_L} \right) \right] K_d^T \approx \left[1 - v_M^h \left(\frac{1}{v_{max}^h} - \frac{1}{k_T^-} \right) \right] K_d^T, \tag{5}$$

$$K_M^P \equiv v_M^s \left[\frac{1}{k_P^-} + \frac{1}{k_s} \left(1 + \frac{k_h}{k_T^-} \right) \right] K_d^P \approx \left[1 - v_M^s \left(\frac{1}{v_{max}^s} - \frac{1}{k_P^-} \right) \right] K_d^P, \tag{6}$$

$$K_M^D \equiv v_M^s \left[\frac{1}{k_D^-} + \frac{1}{k_s} \left(1 + \frac{k_h}{k_T^-} \right) \right] K_d^D \approx \left[1 - v_M^s \left(\frac{1}{v_{max}^s} - \frac{1}{k_D^-} \right) \right] K_d^D. \tag{7}$$

The equilibrium constant is given by $K_e \equiv K_e^b e^{-\Delta G/k_B T}$, where $K_e^b \equiv K_d^T/(K_d^D K_d^P)$ and the dissociations constant are $K_d^I = k_I^-/k_I^+$ with the subscript I=T, D, P respectively. The equilibrium constant varies exponentially with p.m.f.

The inhibitions between substrates and products are complicated because ATP or ADP/P_i binds competitively to the same "open" site no matter the motor functions as a synthase or hydrolase. For convenience, we express the inhibitions in an uncompetitive hydrolysis form with the parameter: $\sigma \equiv 1 + [P]/K_I^{TP} + [D]/K_I^{TD} + [D][P]/K_I^{TDP}$, where $K_I^{TP} \equiv K_d^P \chi k_D^-/k_P^-$, $K_I^{TD} \equiv K_d^D \chi k_P^-/k_D^-$, $K_I^{TDP} \equiv K_d^D K_d^P \chi/[1 + e^{\Delta G/k_B T}]$, and $\chi = e^{\Delta G/k_B T} k_L/v_M^h$.

Eq.(2) implies that the motor is a synthase if $r_c > 0$, a hydrolase if $r_c < 0$, and at equilibrium if $r_c = 0$. Fig.2(b) shows the reversible rotational speed of the motor versus ATP concentration and p.m.f. The motor functions as a synthase only if the ATP concentration is lower than a critical value such as 100μM and p.m.f is higher than 175mV. On the other hand, it becomes a hydrolase when [T]$>$ 100μM and p.m.f$<$ 175mV. The surface in Fig.2(b) also shows the sigmoid kinetics with respect to ΔpH at different Q(Junesch & Gräber, 1987; 1991). The relation between k_h/k_s and ΔpH and damping coefficient of "rotor" can be determined by a stochastic mechanochemical coupling model(Li et al., 2009; Shu & Shi, 2004; Shu & Lai, 2008; Shu et al., 2010)

2.2 Dynamics of system with rotary motor and battery

Recently, F_oF_1 motor is usually reconstituted in liposomes to investigate the H^+/ATP with pH clamp(Steigmiller et al., 2008; Toei et al., 2007; Turina et al., 2003). The dynamics of the system composed of motor and vesicle is urgent. Here we propose a possible experimental situation to study the dynamics of the F_oF_1 motor and vesicle system. In CF_oF_1-liposome experiments, a single purified H^+-translocating ATP synthase from chloroplast can be reconstituted on a vesicle. If the F_1 is extended inside and the vesicle is impermeable except for the proton channel in F_o, how long does the system take to achieve equilibrium once the outside pH is disturbed? This question involves the dynamics of the system and seems too complicated to be solved. However, if the diffusions of the substrates and proton in buffer are rapid enough, i.e., the time that the system takes to achieve steady concentrations of substrates and proton inside is much less than the rate-limiting rotational step, the dynamics of this system can be directly derived form Eqs.1 with different initial conditions as shown in Fig.3. Here, we assumed that the rate-limiting rotational step is equal to the rate of ATP hydrolysis/synthesis and may approximately be calculated from Refs(Shu & Lai, 2008; Shu et al., 2010)

Here, we only need to estimate the upper limit of the ATP diffusion time since ATP is the biggest molecule involved with radius $\sim$ 0.7 nm(Ravshan & Yasunobu, 2004). The distance to be covered is, therefore, at most, the radius of the vesicle which has been taken to be $R_v = 350$ nm. With a free diffusion coefficient of $D_A = 0.3 \times 10^9$ nm^2/s, The most diffusion time of ATP may be estimated as $t_A = R_v^2/(6D_A) = 0.06$ ms. This is two orders of magnitude shorter than the time spent for one ATP synthase even at maximum rate. Although this analysis describes a three-dimensional free diffusion, it gives a reasonable estimate for the particular confined geometry when ATP has explored the whole inside of the vesicle and found the corresponding binding site.

Fig.3 shows the dynamics of F_oF_1 in such a vesicle system calculated from our model. The synthesis/hydrolysis rate achieves a maximum value at 0.1 ms for initial conditions of $P_{EDP} = 1.0$ or $P_{ET} = 1.0$ respectively. After 10 ms, the system enters the steady state. The dynamics is constant with the kinetics values (symbols) and is independent of initial conditions. The rotational rate and inside pH decrease with time, while the ATP concentration

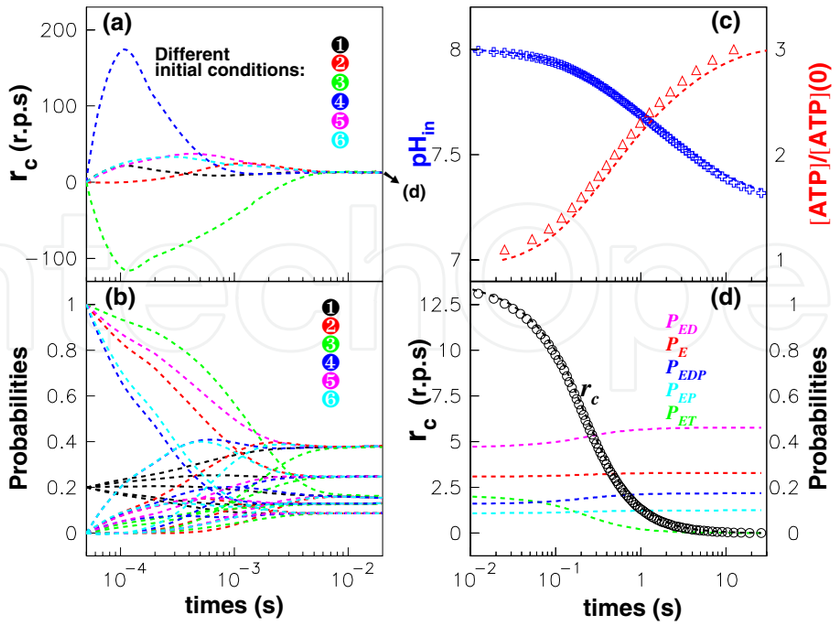

Fig. 3. Dynamics of F_oF_1 motor embedded in a vesicle system. (a) and (b): Evolutions of rotational rates and probabilities with six different initial conditions before 0.02 seconds. (c) Evolutions of pH and ATP concentrations inside. (d) Evolutions of rotational rates and probabilities after 0.01 seconds. The outside pH is constant (=6), while initial inside pH=8, [T]=100 nM, [D]=100 μM, and [P]=1 mM. The diameter of vesicle is 700 nm(Shu & Lai, 2008).

increases monotonically as expected. Here, we do not consider the influence of pH on the activity of F_1. These dynamical predictions can be tested in future experiments.

3. δ-free F_oF_1 rotary motor

An important feature of the two coupled rotary motors is that their stators are rigidly united by b_2 and δ subunits, in which δ subunit connects b_2 and $\alpha_3\beta_3$ crown. Once the δ subunit is deleted, the $\alpha_3\beta_3$ crown stators is no longer constrained, while another stator is still fixed in membrane. Therefore, the $\alpha_3\beta_3$ crown will accompany the "rotor" on rotation, and the transmembrane electrochemical energy is the only power. This is named δ free F_oF_1 rotary motor. On the other hand, chromatophore vesicles are small lipid vesicles that are differentiated to host only the photosynthetic apparatus. These vesicles are closed units, separated from their environment. The the photosynthetic apparatus convert light energy into transmembrane electrochemical energy. The chromatophore vesicle, thus, functions as a rechargeable battery.

We had developed a method to reconstitute the δ free F_oF_1 rotary motor into chromatophore vesicle so that the motor is an ideal self-driven nano-machine(Moriyama et al., 1991; Zhang et al., 2005). Employing a fluorescent actin filament attached to the β-subunits, we have directly observed the light-driven rotation of δ free F_oF_1 rotary motor at single molecule level(Zhang et al., 2005). If the fluorescent actin filament is replaced by a propeller, the motor becomes a self-propelled nano-machine and can serves for nano-submarine in artery to promote thrombolysis. Furthermore, if we exchange an antibody for the fluorescent actin

filament, the self-driven nano-machine can detect antigen because it will slowdown due to damp increasing caused by antigen binding. The speed decreasing can be detected by measuring the rate varying of inside pH of chromatophore. Thus, δ free F_oF_1 rotary motor has a great potential to be developed into a biosensor and activator for different applications.

3.1 Reconstitution of δ-free F_oF_1 motor

Purification of the β-subunit, F_1 ($\alpha_3\beta_{(10\times his\text{-}tag)3}\gamma$), and F_oF_1-ATPase: The F_1-ATPase coding sequence was isolated from thermophilic bacterium PS3, site-directed mutations of a cys193ser and gamaser107cys were introduced, and a 10 *histidine* tag was inserted downstream of the initiation codon. The mutated construct, pGEMMH, was then cloned into the expression plasmid pQE-30, and the expression plasmid pQE-MH was inserted into *E. coli* JM103(*uncB-UncD*) in which a majority of F_1-ATPase genes have been eliminated. Thermophilic bacterium, *Bacillus* PS3$\beta_{10\times his\text{-}tag}$ subunit ($TF_1\beta$), and F_1-ATPase ($\alpha_3\beta_{(10\times his\text{-}tag)3}\gamma$) were expressed and purified as Ref.(Yang et al., 1998), in which the JM103 strain expressing F_1-ATPase was cultured in 2× YT medium (AMP^+) for 3-4 h at 37°C. When the A_{660} increased to 0.6-0.8, the expression of the F_1-ATPase was induced by addition of 1 mmol/L isopropylthio-β-D-galactoside for 3 h. Cells were harvested by centrifuging for 15 min at 4000g and cell extractions were prepared using lysozyme (1 mg/mL)/sonication (5 min) in 50 mmol/L Tris-HCl (pH 8.0) buffer containing 0.5 mol/L NaCl and 1 mmol/L phenylmethane sulfonyl fluoride. The extracts were incubated at 60 °C for 30 min, and $TF_1\beta$ was purified using Ni^{2+}-NTA affinity chromatography at 4 °C. F_1-ATPase ($\alpha_3\beta_{(10\times his\text{-}tag)3}\gamma$) was purified as Ref.(Montemagno & Bachand, 1999) at 25 °C. The F_oF_1-ATP synthase from the *E. coli* JM103(*uncB-UncD*) was purified as Ref.(Yang et al., 1998). The mutant ATP synthase containing the His-tag could be isolated with Ni-NTA column. F_oF_1-ATPase was eluted with buffer B containing 0.05% lysolecithin and 250 mM imidazole at 4 °C, and then further purified by a gel filtration column (Superdex 200 HR 10/30 Pharmacia). The purified protein was analyzed by SDS-PAGE.

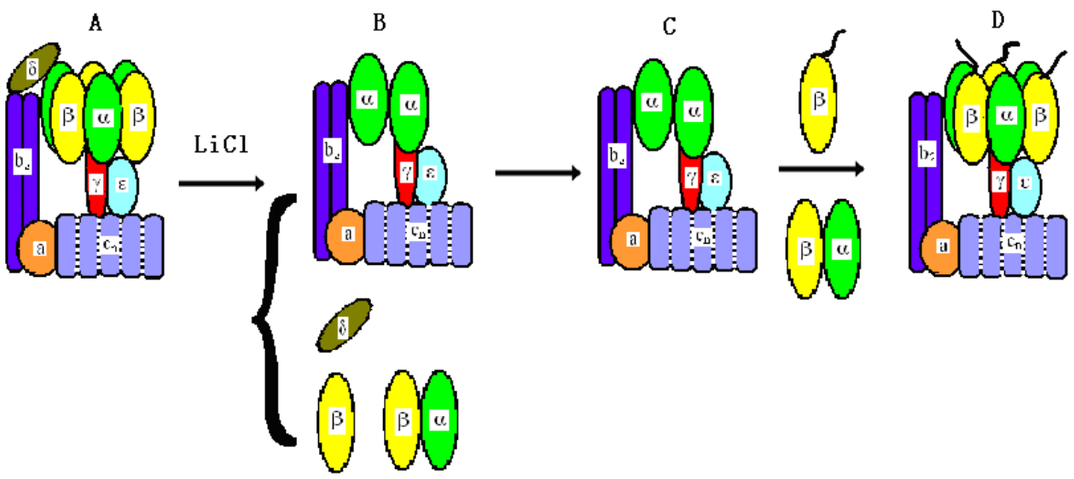

Fig. 4. The procedure of reconstitution of δ-free F_oF_1-ATPase motor. (A) F_oF_1-ATPase; (B) F_oF_1-ATPase is treated by LiCl to remove δ subunit; (C) Rebinding of purified β and α subunits; (D) The reconstituted δ-free F_oF_1-ATPase motor(Zhang et al., 2005).

The procedure of δ-subunit deletion of F_oF_1-ATPase is briefly shown in Fig.4. The proteoliposome containing F_oF_1-ATPase and bacteriorhodopsins (BRs) was incubated with 2 M LiCl, 0.1 mM Tricine-NaOH, 10 mM $MgCl_2$, and 1 mM ATP for 20 min at 4 °C. Then the proteoliposome was washed and isolated by centrifuging. Because some α and β subunits may be removed during δ delation, the LiCl-treated proteoliposome needs incubating with purified $\alpha_3\beta_3\gamma$(or β) subunits at 4 °C for 60 min (for each divided subunit of F_1 with buffer 0.1 mM Tricine-NaOH, 10 mM $MgCl_2$, 50 mM KCl, 0.5 mM NaCl, and 1 mM ATP), and then is cultured at 37 °C for 60 min (for reconstituting of δ-free F_oF_1-ATPase). The proteoliposome needs to be isolated to obtain the reconstituted δ-free F_oF_1-ATPase(Liao et al., 2009; Su et al., 2006; Tao et al., 2008).

3.2 Direct observation of the light-driven rotation of the δ-free F_oF_1 motor

Preparation of motor and liposome: F_oF_1-ATPase from the *E. coli* JM103(*uncB-UncD*) was purified as Ref.(Yang et al., 1998). The purified BR and F_oF_1-ATPase were co-reconstituted into a liposome. The liposome was prepared by reverse-phase evaporation with the mixture of soybean lipid and 1,2-dipalmitoyl-sn-glycero-3 phosphoethanolamine-N-biotinyl (molar ratio: 7:0.001)(Matsui & Yoshida, 1995). The molar ratio of BR and F_oF_1-ATPase was about 100:1, and that of lipids and protein was 30:1(w/w), so that it is possible for one proteoliposome to contain one F_oF_1-ATPase and more than 20 BR molecules.

Preparation of fluorescent actin filaments: The G-actin was co-labeled with FITC and Maleimido-C3-NTA-Ni^{2+} in buffer (50 mM Hepes-KOH, pH 7.6, 4 mM $MgCl_2$, and 0.2 mM ATP) for one night at 4 °C. The free FITC and Maleimido-C3-NTA (Ni-NTA) were removed by a desalting column. Then the labeled G-actin was polymerized in buffer containing 50 mmol/L Hepes-KOH (pH 7.6), 50 mmol/L KCl, 4 mmol/L $MgCl_2$, and 2 mmol/L ATP.

Preparation for immobilization of proteoliposomes in the experimental system for observation. Biotin-AC5-Sulfo-OSu was linked to the polylysine which had previously coated on the bottom of the dishes, and then 100 μl of 10 nM streptavidin was added into the dish bottom. After 5 min, the free streptavidin was washed. The proteoliposomes were conjugated by lipid-biotin-streptavidin-biotin-polylysine to the glass surface. And then the FITC-labeled F-actin filaments were attached to theβ-subunit of F_1 part through the His-tag with Maleimido-C3-NTA, as a marker of orientation for observation under an Olympus IX71 fluorescent microscope equipped with an ICCD camera.

To visualize the rotation of F_o in proteoliposome, a fluorescent actin filament was attached to β subunits through His-tag, while the proteoliposome was immobilized onto the glass surface through the biotin- streptavidin-biotin complexes(Fig.5A). The sample was exposed under the 570 nm cool light for 30 min to initiate the rotation of the F_o motor. Before illumination, the buffer containing 2 mM NaN_3 and 2 mM ADP was infused into the chamber. The clockwise rotation of actin filament was traced directly by an Olympus IX71 fluorescent microscope equipped with an ICCD camera (Roper Scientific, Pentamax EEV 512×512 FT) viewing from F_o side to F_1. Fig.5B shows an example of the sequential clockwise rotation images with 100 ms interval. We have selected six rotational data with different length filaments to show in Fig.5C. The rotation displays occasional pause or even backwards due to Brownian fluctuation. The rotation speed decreases with the length of filament increasing, which is in agreement with the results of single molecule experiments of F_1Noji et al. (1997); Yasuda et al. (1998) as expected. In addition, several control experiments were performed to confirm that the observed rotation is driven by transmembrane proton flow. As shown in Fig.5D, the rotation stopped immediately once 5 μl of 10 μM CCCP was added. It was also found that if the

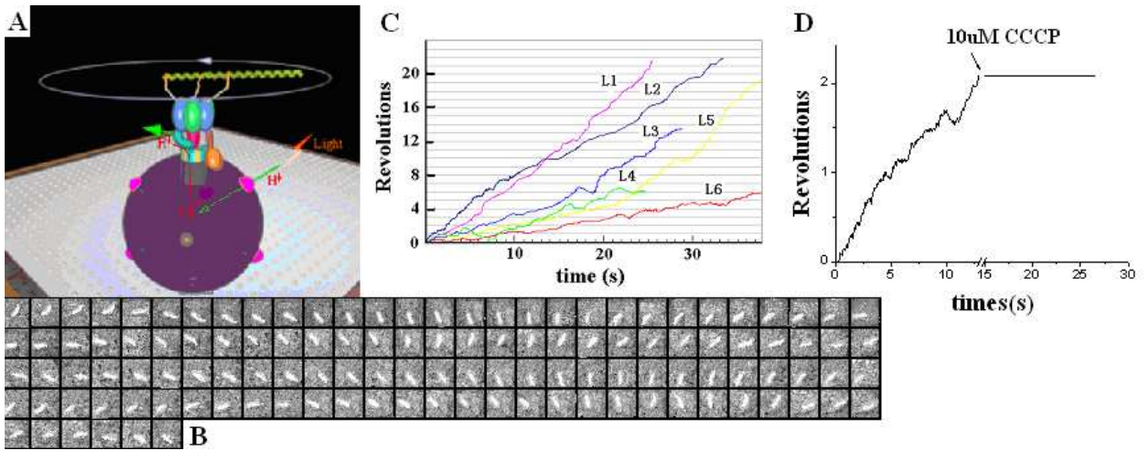

Fig. 5. (A)The system used for observation of the F_o rotation in the proteoliposome which was immobilized on the cover glass with biotin-streptavidin-biotin. (B)The sequential images of a clockwise rotating fluorescent actin filament. Time interval is 100 ms. (C)Time courses of the actin filament rotation with different length. The fluorescent filament was attached to the β subunits through His-tag. The length of filaments denoted L1,L2,L3,L4,L5 and L6 are 1.7, 1.9, 2.0, 2.3, 2.8 and 3.3 μm respectively. (D)The rotation was inhibited by adding CCCP, which verified the motor was indeed driven by transmembrane ΔpH(Zhang et al., 2005).

sample is in dark or is incubated with DCCD before illumination, no rotation has been observed (data are not shown) because CCCP destroyed the transmembrane p.m.f and DCCD blocked the proton channels. Furthermore, if NaN_3 and ADP disappeared in the buffer, no rotation of filament was found because NaN_3 and ADP prevented the $\alpha_3\beta_3$ crown from sliding to γ subunit(Muneyuki et al., 1993). These results demonstrated that the rotation of filaments depended on the p.m.f produced in proteoliposome. It is interesting that the ΔpH transmembrane of proteoliposome can persist for a long time. After the illumination, some filaments rotated continuously more than 20 min. The proteoliposome function as a recharge battery to supply energy to the rotary motor.

4. Biosensor developed by δ-free F_oF_1 motor

Light-driven electron transfer causes the proton gradient across the membrane and leads the proton flux through n channels(c_n) in F_o. The interaction between a subunit and proton flux generates the relative movement between a subunit and c ring. Proton flux will simultaneously alter the inside and outside pH of chromatophore. It is well established that the rotational speed of motor is tightly coupled to the rate of proton transmembrane transport, that is, the changing of speed is equivalent to the altering of proton transfer rate. On the other hand, motor speed can be regulated by changing the load, while the pH altering can be detected by pH-sensitive fluorescent probes such as QDs (quantum dots)(Deng et al., 2007). Thus, the nanomachine can be developed as a sensitive biosensor if the rotor is linked antibody/complementary strand and pH-sensitive probes are labeled outside (or inside) chromatophore.

5. Protein or virus detector

The first type of rotary biosensor was based on the antibody-antigen reaction to capture virus or specific protein. The nanomachine was constructed as shown in Figure6(a): β subunit(1) was linked by its antibody(2), while the antibody(4) of H9 avian influenza virus was connected to β antibody(2) in series by biotin-streptavidin-biotin (3). The chromatophore(6) with F_oF_1 -ATPase was hold on glass surface(7) coated with chitosan. If H9 avian influenza virus(5) exist, they will load to the motor through antibody-antigen reactions. Virus or protein loading, therefore, change motor speed. The speed changing can be detected by monitoring the fluorescent intensity indicated by pH-sensitive dye (or QDs). That is, the fluorescent intensity altering can be used to indirectly detect virus or protein. Its signal-to-noise ratio can be distinguished at single molecular level. Thus, this nanomachine may be a convenient, rapid, and even super-sensitive for detecting virus/protein particles.

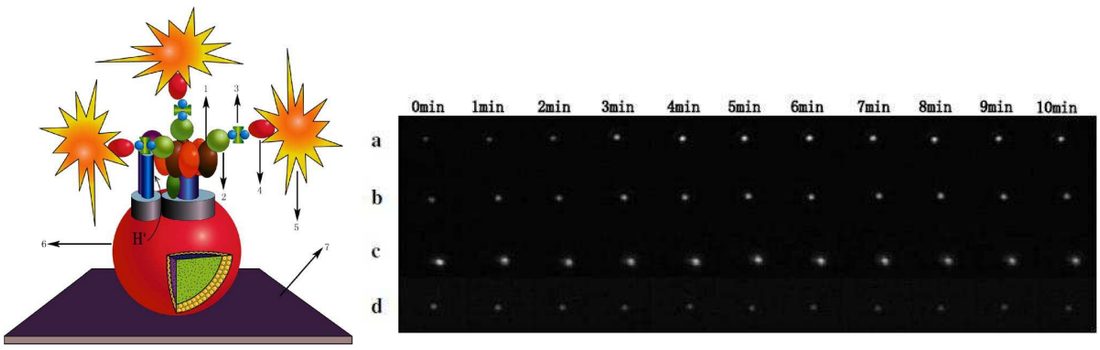

(a) Cartoon of detector (b) The course of fluorescence intensity

Fig. 6. (a) Basic design of biosensor based on δ-free F_oF_1. The fluorescence probe F1300 labeled inside of chromatophores was used as a proton flux indicator. **1** β subunit; **2** antibody of β subunit; **3** the complex of biotin-streptavidin-biotin; **4** the antibody of H9 avian influenza virus; **5** H9 avian influenza virus; **6** chromatophore; **7** glass surface coated with chitosan. (b) Images of intensity change of fluorescence dots caused by pH changing inside chromatophore in the course of 10 min. **a** with virus; **b** without virus; **c** with two antibodies; **d** without ADP(Liu et al., 2006b).

Preparation of H9 avian influenza virus: The avian H9 influenza were propagated in the allantoic cavities of 11-day-old embryonated chicken eggs at 37 °C for 3 days. The allantoic cavities were collected and centrifuged at 4000 rpm for 40 min and then the supernatant was centrifuged again at 100,000g for 2 h. The viruses were resuspended in PBS buffer and used in the experiments.

Labeling of fluorescence probe: The fluorescence probe F1300 was labeled into chromatophore as follows: 3 μl F1300 (0.0015 mol/L, dissolved in ethanol) was added to 150μl chromatophores and then was ultrasonicated in ice for 3 min to make the probe into inner chromatophores. The free fraction was washed by centrifugation at 12,000 rpm for 30 min at 4 °C three times. The precipitate was resuspended in tricine-NaOH buffer.

6. DNA or RNA detector

The second type of rotary biosensor was based on base-pair reaction to capture nucleic acid sequences such as DNA or RNA. Specific RNA/DNA probes, which are the complementary

strand of target RNA/DNA, were linked to each β subunits of nanomachine. Once base-pair reaction take places between two strands, the flexible probes will transform into a rigid rods so that motor will slowdown because the damp of rigid rod is much larger than that of flexible single chain. Detection of RNA/DNA was based on the proton flux altering induced by light-driven rotation of δ-free F_oF_1 motor. The base-pair reaction was indicated by changing in the fluorescent intensity of pH-sensitive CdTe quantum dots. Our results showed that the assay was so sensitive (1.2×10^{-18}M) that it can distinguish the target miRNA family members. Moreover, the method could be used to monitor real-time base-pair reaction without any complicated fabrication. The nanomachine has a great potential of clinical application of RNA/DNA.

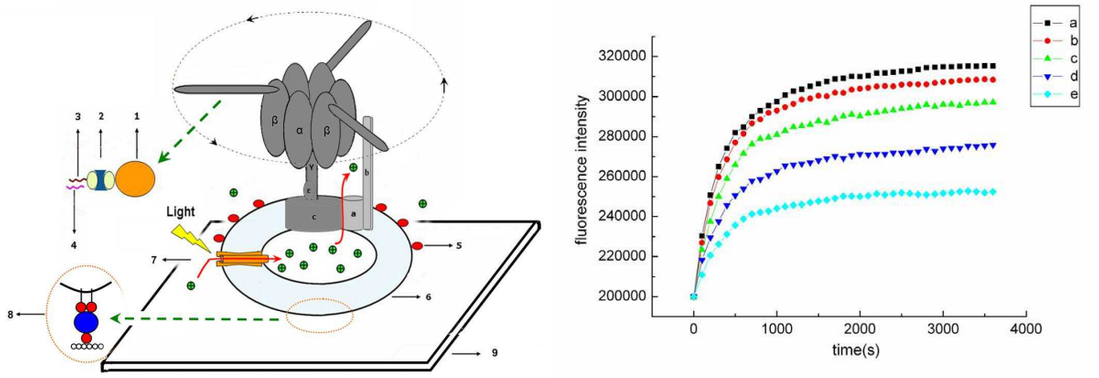

(a) Cartoon of detector. (b) Results of different concentration of miRNA.

Fig. 7. (a)Schematic diagram of the biosensor based on δ-free F_oF_1-ATPase embedded chromatophore. 1, 2, 3, 4, 5, 6, 7, 8, and 9 represent the antibody against β subunit, the linking complex composed of [biotin-AC5-sulfo-OSu]-streptavidin-[biotin-AC5-sulfo- OSu], miRNA probe, target miRNA, 535nm QDs, chromatophore, bacteriorhodopsins (BRs), the linking system of lipid-biotin-streptavidin-[biotin-AC5-sulfo-OSu]-Polylysine, and the glass surface, respectively. (b)Results of different concentration of miRNA. RNA was extracted from MCF-7 cells. **a** without RNA; from **b** to **e** the amounts of miRNA was summed from $10, 10^2, 10^4$ and 10^6 cells respectively. Base-pair reaction was hold at 37°C(Liao et al., 2009).

The chromatophores (100 μL) were resuspended in buffer A (50mM tricine-NaOH, 5mM $MgCl_2$, 10mM KCl, pH 6.5) and incubated for 3 h at room temperature with 100 μL CdTe QDs ($1\times10^{15}/\mu$L, dissolved in water)(Zhang et al., 2007). Free QDs were washed away by centrifuging at 13 000 rpm for 30 min at 4 °C in three times. The precipitate (QD-labeled chromatophores) was resuspended in 100 μL of 50mM tricine buffer (pH 6.5). Meanwhile, 2 μL of 2 μM biotin was added in 20 μL β subunit antibody at room temperature for 30 min, followed by adding 2 μL of 2 μM streptavidin at room temperature for 30 min. The streptavidin-biotinlabeled β-subunit antibody was incubated with 5 μL QDs labeled chromatophores fixed on the glass slips at 37°C for 1 h. Redundant free biotin-streptavidin-labeled β-subunit antibody was rinsed with 50mM TSM buffer (50mM Tricine-NaOH pH 7.0, 0.25M sucrose, and 4mM $MgCl_2$). Then 100 μL 10μM miRNA probe labeled with biotin was added and incubated at room temperature for 30 min. Free probes were washed out by 50mM TSM buffer. The δ-free F_oF_1-ATPase with chromatophore was immobilized on the glass surface through the biotin-streptavdin-biotin. miRNA probe system was hybridized with miRNA target in 100μL formamide hybridization solution at 37°C.

Before the detection, the sample was exposed under the 570 nm cool light for one hour to initiate the rotation of the F_oF_1-ATPase. During illumination, the buffer containing 2mM NaN_3 and 2 mM ATP was infused into the chamber to inhibit the hydrolysis activity of the F_oF_1-ATPase and prevent relative sliding between $\alpha_3\beta_3$ crown and γ subunit.

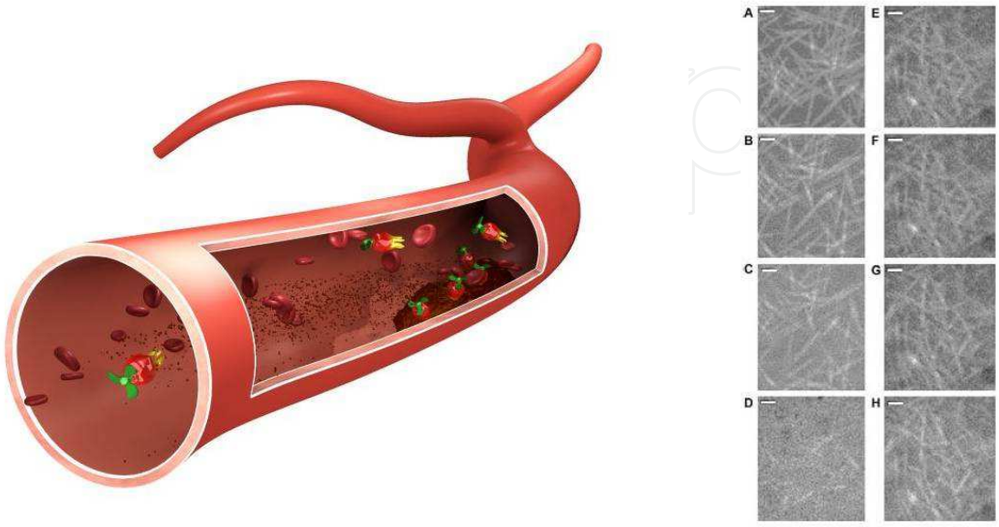

(a) Cartoon of submarine cruising in artery to promote thrombolysis. (b) Results of experiment *in vitro*.

Fig. 8. (a) Cartoon of submarine cruising in artery to promote thrombolysis. (b) Results of experiments *in vitro*. Left row (A-D) represents the course of fibrinolysis in 30 min with lumbrokinase and δ-free F_oF_1 motor, while right row (E-H) does that of fibrinolysis in 30 min only with lumbrokinase(Tao et al., 2008).

7. A potential activator to promote thrombolysis

Cardiovascular disease such as ischemic stroke is a substantial cause of morbidity and mortality. The primary aim of thrombolysis in acute ischemic stroke is recanalization of an occluded intracranial artery. Recanalization is an important predictor of stroke outcome as timely restoration of regional cerebral perfusion helps salvage threatened ischemic tissue. At present, intravenously administered tissue plasminogen activator (IV-TPA) remains the only FDA-approved therapeutic agent for the treatment of ischemic stroke within 3 hours of symptom onset. Recent studies have demonstrated safety as well as efficacy of IV-TPA even in an extended therapeutic window. However, the short therapeutic window, low rates of recanalization, and only modest benefits with IV-TPA have prompted a quest for alternative approaches to restore blood flow in an occluded artery in acute ischemic stroke. Although intra-arterial delivery of the thrombolytic agent seems effective, various logistic constraints limit its routine use and as yet no lytic agent have not received full regulatory approval for intra-arterial therapy. Mechanical devices and approaches can achieve higher rates of recanalization but their safety and efficacy still need to be established in larger clinical trials(Sharma et al., 2010). The δ-free F_oF_1 motor has a potential to be designed a self-driven nanomachine, which serve as a submarine cruising in artery to promote thrombolysis. Our

experiment *in vitro* has demonstrated that the motor may be one of alternative approaches to restore blood flow in an occluded artery in acute ischemic stroke. However, the mechanism of promoting thrombolysis has not been uncovered.

FITC Labeling on fibrinogen and fibrin formation: Fibrinogen (1 ml, 0.03 mM) was dissolved in PBS buffered saline containing 137 mM NaCl, 3 mM KCl, 8 mM Na_2HPO_4, 1 mM KH_2PO_4, pH 8.5. FITC was added to the fibrinogen solution under intensive stirring to a final concentration of 50 mg/ml(Sakharov et al., 1996). The fibrin fiber obtained from fibrinogen was polymerized with thrombin (0.5 U/μl) and fixed on the glass surface. After incubation at 37 °C for 30 min, a fibrin network with an approximate length of 200 μm was formed.

Fig.8(b) shows the morphological features of the fibrinolysis process observed directly under a fluorescence microscope. At the outset, two fibrin networks A and E, including fiber size, density, and branch point density, were similar. However, promotion of the fibrinolysis by δ-free F_oF_1 motor can be observed by comparing left and right rows. After 30 min, the fibrin almost disappear due to δ-free F_oF_1 motor (D), while the control one (H) still partly exist. It can be imaged that the many self-driven nanomachines will specially bind to fibrin and promote thrombolysis because of cooperative effect of collective propellers.

8. Self-assembly of ghost with the nanomachine

Nanotechnology aims to construct materials and operative systems at nanoscale dimensions. Several potential applications can be envisioned: targeted drug delivery systems, tissue engineering scaffolds, photonic crystals, and micro/nano fluidic and computational devices. The fundamental challenge in nanotechnology is to construct systems with varied functional features and predictably manipulate processes at the nanometer length scale. Conventional construction methods based on photolithography can successfully generate two-dimensional structures using a "top-down" approach, in which patterned surfaces are prepared by etching with light. Feature sizes on the order of 50 nm are easily achieved with commonly available technologies. Advances in specialized lithographic techniques (e.g. scanning probe lithography) have extended the resolution to below 20 nm. Molecular self-assembly serves as an alternative paradigm for preparing functional nanostructures, is perhaps one of the most intriguing phenomena in the fields of chemistry, materials, and bioscience, as well as is characterized by spontaneous diffusion and specific association of molecules dictated by non-covalent interactions. There are numerous recent examples involving different molecular entities: organic molecules, proteins, peptides, DNA and molecular motors(Kumar et al., 2011; Lo et al., 2010; Rajagopal & Schneider, 2004; Tao et al., 2009; Yin et al., 2008; Zhao et al., 2010).

A current challenge in molecular self-assembly is to achieve controlled organization in three-dimensions, to provide tools for biophysics, molecular sensors, enzymatic cascades, drug delivery, tissue engineering, and device fabrication. Ghosts (Erythrocyte membranes) are promising bioactive materials and have a great potential of application in drug delivery. The ghost is a kind of flexile membrane, composed of a lipid bilayer and cytoskeleton. One of special shapes is concave disk with the diameter about 8 μm and the thickness about 1.7μm respectively. Ghosts loaded with drugs or other therapeutic agents have been exploited extensively, owing to their remarkable degree of bio-compatibility, biodegradability, and a series of other potential advantages. We have been motivated to design a novel self-organized material using ghosts with δ-free F_oF_1 motor. A lot of interesting phenomena appear: Most chromatophores combined with δ-free F_oF_1 motor arrayed in a filament-like fashion through biotin-streptavidin-biotin interaction. The filament-like nanomachines were able to stick

around the surface of the ghost with the F_1 part against the ghost. Moreover, many ghosts, which were stuck around by filament-like nanomachines, assembled spontaneously to a larger scale complex with two or three layers. This sandwich structure may be useful for the self-driven delivery of drugs or other therapeutic agents.

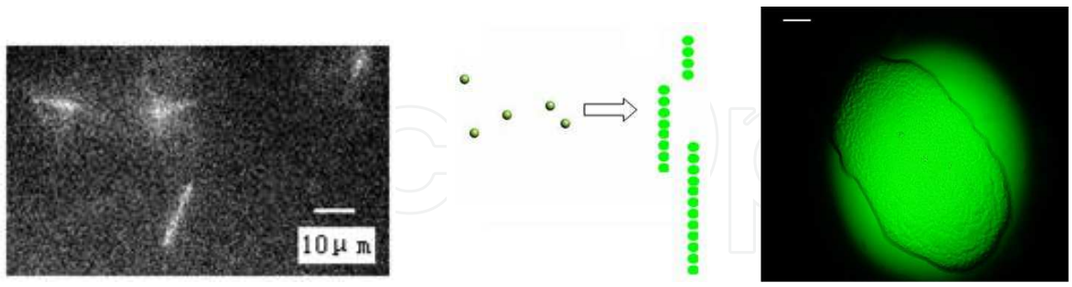

(a) Micrograph of chromatophore-filaments.

(b) Possible mechanism of self-assembly of filament.

(c) Micrograph of larger scale assembly structure.

Fig. 9. (a) Self-assembled filaments of δ-free F_oF_1 motors observed by fluorescence microscopy. (b) Possible mechanism of self-assembly of filament. Green ball represents individual δ-free F_oF_1 motor with chromatophore. Green lines represent chromatophores linked through biotin-streptavidin-biotin into filament structures. Scale bar represents 10 μm. (c) Micrograph of larger scale assembly structure. Ghosts with fluorescence-labeled δ-free F_oF_1 motors aggregate together and self-assemble into a large structure about 0.6 mm $\times$ 1.2 mm in size, which is stable for more than one week.(Tao et al., 2009).

Here, we present a novel type of self-assembled complex consisting of filaments of chromatophores with δ-free F_oF_1-ATPases and ghost, the detailed structure of which was observed by fluorescence microscopy and confocal microscopy. In the absence of light, biotin-labeled chromatophores embedded F_oF_1-ATPase are joined together by streptavidin to form filaments. These filaments can attach to ghost surface, such that the ghosts will aggregate into a larger scale self-assembled complexes with two or three layers, held together in head to head fashion between the rotary F_1's. However, if the complex is illuminated, it will disassemble due to rotation of F_1 caused by light energy. The diameter of these macroscopic complexes is more than 1 mm. δ-free F_oF_1-ATPase act as a switch to control the ghosts' self-assembly and self-disassembly, while the remote control signal (power) is light. This system, thus, has a great potential to be developed into a controllable micronmachine of drug delivery.

Ghost Preparation: Fresh blood of pig was washed three times with cold 0.15 M NaCl buffer, pH 8.0, and plasma and leukocytes were discarded. Ghosts were obtained by hypotonic lysis. Red blood cells were obtained from fresh blood and washed three times with PBS buffer (isotonic phosphate-buffered saline, pH 8.0). The washed cells were added to 40 volumes of ice-cold 5P8 buffer (5 mM sodium phosphate, pH 8.0) and left at room temperature for 20 min before centrifuging at 20 000g for 1 h at 4 °C. The pale ghost layer was collected and washed three more times with lysis solution(Steck et al., 1970).

Observation of Self-Assembly: Ghosts attached chromatophore-filaments were resuspended in 40 volumes of ice-cold buffer (0.5 mM sodium phosphate, pH 7.6) for 1 h. Addition of 5 mM NaN_3, 2 mM $MgCl_2$, 50 mM KCl, and 2 mM adenosine 50-diphosphate (ADP) to the buffer created conditions for light driven rotation of δ-free ATPase within the ghosts. The complexes were put into a cell, in which the chromatophores were illuminated by 570 nm

light for 30 min at 4 °C. This illumination initiated proton transfer across the membrane of the chromatophores, and the rotation of δ-free F_oF_1-ATPase was then driven by the p.m.f. Once proton transfer was initiated, the cell was incubated at 37 °C throughout the whole experiment. The self-assembly and self-disassembly process was observed with an Olympus IX71 fluorescence microscope and recorded with a digital CCD camera (iXon CCD, ANDOR Technology). Confocal microscopy (Olympus FV500, optical scanning confocal microscope) was used during the scanning process of multiple layers of self-assembled complexes. FV1000 software was used to reconstruct the three-dimensional images.

9. Conclusion

In contrast to human-made machines, protein motors are self-assembled by natural biomaterial or elements, and operate in a world where Brownian motion and viscous forces dominate. The relevant energy scale is k_BT, which amounts to 4 pN·nm. This may be compared to the $\sim$ 80 pN·nm of energy derived from hydrolysis of a single ATP molecule at physiological conditions. Thermal, nondeterministic motion is thus an important aspect of the dynamics of molecular motors.

ATP hydrolysis does spontaneously occur in F_1, whereas the thermodynamically unfavorable reaction, ATP synthesis, has to be driven by harnessing the transmembrane proton flow in F_o. The mechanism of ATP formation in the F_1 part is well described by the "binding change mechanism". This has been developed in great detail by many techniques, and understanding of the mechanism has been claimed to be "almost complete". However, if the motor functions as a synthase, the two substrates, ADP and P_i, are recombined into one product, ATP. The binding order of the two substrates is still unclear(Watanabe et al., 2010). Another challenging question is whether the main kinetic enhancement occurs upon filling the second or the third site(Boyer, 2000; Milgrom & Cross, 2005; Senior et al., 2002). For F_o, the torque generation between a and c_n in F_o is still covered(Pogoryelov et al., 2010). In addition, it has remained unsettled whether the entropic (chemical) component of $\Delta\tilde{\mu}_{H^+}$ relates to the difference in the proton activity between two bulk water phases (ΔpH^B) or between two membrane surfaces (ΔpH^S)(Cherepanov et al., 2003).

It is of interest to ponder whether we can employ F_oF_1-ATPase nanomachine in artificial environments outside the cell to perform tasks that we design to our benefit(Martin et al, 2007)? One striking demonstration is the construction of a nickel nanopropeller that rotates through the action of an engineered F_1-ATPase motor(Soong et al., 2000). A metal-binding site was engineered into the motor and acted as a reversible on-off switch by obstructing the rotation upon binding of a zinc ion(Liu et al., 2002), similar to the action of putting a stick between two cogwheels. The other high light examples are the sol-gel packaging of vesicles containing bacteriorhodopsin, a light driven proton pump, and F_oF_1-ATP synthase(Choi & Montemagno, 2005; Luo et al., 2005), or F_oF_1-ATPase embedded chromatophore(Cui et al., 2005). Upon illumination, protons are pumped into the vesicles and ATP is created outside the vesicle by the ATP synthase. Besides the excellent stability of these gels (bacteriorhodopsin continued functioning for a few months), this technology provides a convenient packaging method and a way to use light energy for fueling devices. Therefore, these nanodevices with a battery can be employed to design a rapid, no labeled, sensitive and selective biosensor(Cheng et al., 2010; Deng et al., 2007; Liu et al., 2006b; Zhang et al., 2007), or construct a self-propelled nano-machine which can serves for nano-submarine in artery to promote thrombolysis(Tao et al., 2008). With ghost, the motor also has a great potential for drug delivery(Tao et al., 2009). Of course, all of these application tries are very coarse,

and little more than proof-of-principle examples. Thus, there are many questions to be investigated for application.

10. Acknowledgements

This work was supported by the National Basic Research Program of China (973 Program) under the grant No. 2007CB935903 and No. 2007CB935901, the National Natural Science Foundation of China (90923009 and 20873176), Knowledge Innovation Program of the Chinese Academy of Sciences (YYYJ-0907), Instrument Program of Chinese Academy of Sciences (07CZ203100), and Starting Mérieux Research Grants 2011-Institute of Biophysics-Prof. JiachangYue.

11. References

Abrahams, J. P.; Leslie, A. G. W.; Lutter, R.; Walker, J. E. (1994). Structure at 2.8 Å resolution of F_1-ATPase from bovine heart mitochondria. *Nature*. 370., 621-628

Adachi, K.; Oiwa, K.; Nishizaka, T.; Furuike, S.; Noji, H.; Itoh, H.; Yoshida, M. & Kinosita, K. Jr. (2007). Coupling of rotation and catalysis in F_1-ATPase revealed by single-molecule imaging and manipulation. *Cell*. 130., 309-321

Aksimentiev, A.; Balabin, I. A.; Fillingame, R. H. & Schulten, K. (2004).Insights into the molecular mechanism of rotation in the F_o sector of ATP synthase. *Biophys. J*. 86., 1332-1344

Ballmoos, C. von; Wiedenmann, A. & Dimroth, P. (2009). Essentials for ATP synthesis by F_1F_o ATP synthase. *Annu. Rev. Biochem*. 78., 649-672

Boyer, P. D.; Cross, R. L. & Momsen, W. (1973). A new concept for energy coupling in oxidative phosphorylation based on a molecular explanation of the oxygen exchange reactions . *Proc. Natl. Acad. Sci. USA*. 70., 2837-2839

Boyer, P. D. (1997). The ATP synthase-A splendid molecular machine. *Annu. Rev. Biochem.* 66.,717-749

Boyer, P. D. (2000). Catalytic site forms and controls in ATP synthase catalysis. *Biochim. Biophys. Acta*. 1458., 252-262

Cheng, J.; Zhang, X. A.; Shu, Y. G. & Yue, J. C. (2010). F_oF_1-ATPase activity regulated by external links on β subunits. *Biochem. Biophys. Res. Commun*. 391., 182-186

Cherepanov, D. A.; Feniouk, B. A.; Junge, W. & Mulkidjanian, A. Y. (2003). Low dielectric permittivity of water at the membrane interface: effect on the energy coupling mechanism in biological membranes. *Biophys. J*. 85., 1307-1316

Choi, H. J. & Montemagno, C. D. (2005). Artificial Organelle: ATP Synthesis from cellular mimetic polymersomes. *Nano. Lett*. 5., 1538-1542

Cui, Y. B.; Fan, Z. & Yue, J. C. (2005). Detecting proton flux across chromatophores driven by F_oF_1-ATPase using *N*-(fluorescein-5-thiocarbamoyl)-1,2-dihexadecanoyl-*sn*-glycero-3-phosphoethanolamine, triethylammonium salt. *Anal. Biochem*. 344., 102-107

Deng, Z. T.; Zhang, Y.; Yue, J. C.; Tang, F. Q. & Weil, Q. (2007). Green and Orange CdTe Quantum Dots as Effective pH-Sensitive Fluorescent Probes for Dual Simultaneous and Independent Detection of Viruses. *J. Phys. Chem. B*. 111., 12024-12031

Diez, M.; Zimmermann, B.; Börsch, M.; König, M.; Schweinberger, E.; Steigmiller, S.; Reuter, R.; Felekyan, S.; Kudryavtsev, V.; Seidel, C. A. M. & Gräber, P. (2004). Proton-powered

subunit rotation in single membrane-bound F_1F_o-ATP synthase. *Nat. Struct. Mol. Biol.* 11., 135-141

Düser, M. G.; Zarrabi, N.; Cipriano, D. J.; Ernst, S.; Glick, G. D.; Dunn, S. D. & Börsch, M. (2009). 36° step size of proton-driven *c*-ring rotation in F_1F_o-ATP synthase. *EMBO J.* 28., 2689-2696

Elston, T.; Wang, H. & Oster, G. (1998). Energy transduction in ATP synthase. *Nature*. 391., 510-513

Feniouk, B. A. & Yoshida, M. (2008). Regulatory mechanisms of proton-translocating F_1F_o-ATP synthase. *Results Probl. Cell Differ.* 45.,279-308

Ishmukhametov, R.; Hornung, T.; Spetzler, D. & Frasch, W. D. (2010). Direct observation of stepped proteolipid ring rotation in *E. coli* F_oF_1-ATP synthase. *EMBO J.* 29.,3911-3923

Itoh, H.; Takahashi, A.; Adachi, K.; Noji, H.; Yasuda, R.; Yoshida, M. & Kinosita, K. (2004). Mechanically driven ATP synthesis by F_1-ATPase. *Nature*. 427., 465-468

Jiang, W. P.; Hermolin, J. & Fillingame, R. H. (2001). The preferred stoichiometry of c subunits in the rotary motor sector of *E. coli* ATP synthase is 10. *Proc. Natl. Acad. Sci. USA*. 98., 4966-4971

Junesch, U. & Gräber, P. (1987). Influence of the redox state and the activation of the chloroplast ATP synthase on proton-transport-coupled ATP synthesis/hydrolysis. *Biochim. Biophys. Acta*. 893., 275-288

Junesch, U. & Gräber, P. (1991). The rate of ATP-synthesis as a function of ΔpH and $\Delta\psi$ catalyzed by the active, reduced H^+-ATPase from chloroplasts. *FEBS. Lett.* 294., 275-278

Junge, W. (2004). Protons, Proteins and ATP. *Photosynthesis Res.* 80.,197-221

Kaim, G.; Prummer, M.; Sick, B.; Zumofen, G.; Renn, A.; Wild, U. P. & Dimroth, P. (2002). Coupled rotation within single F_1F_o enzyme complexes during ATP synthesis or hydrolysis. *FEBS Lett*. 525., 156-163

Kothen, G.; Schwarz, O. & Strotmann, H. (1995). The kinetics of photophosphorylation at clamped ΔpH indicate a random order of substrate binding. *Biochim. Biophys. Acta.* 1229., 208-214

Kumar, P.; Pillay, V.; Modi, G.; Choonara, Y. E.; du Toit, L. C.& Naidoo, D. (2011). Self-assembling peptides: implications for patenting in drug delivery and tissue engineering. *Recent Pat Drug Deliv. Formul.* 5., 24-51

Li, M.; Shu, Y. G. & Ou-Yang, Z. C. (2009). Mechanochemical Coupling of Kinesin Studied with a Neck-Linker Swing Model. *Commun. Theor. Phys.* 51., 1143-1148

Liao, J. Y.; Yin, J. Q. & Yue, J. C. (2009). A novel biosensor to detect microRNAs rapidly. *Journal of Sensors*. 2009., 671896

Liu, H. Q.; Schmidt, J. J.; Bachand, G. D.; Rizk, S. S.; Looger, L. L.; Hellinga, H. W. & Montemagno, C. D. (2002). Control of a biomolecular motorpowered nanodevice with an engineered chemical switch. *Nat. Mater*. 1., 173-177

Liu, X. L.; Zhang, X. A.; Cui, Y. B.; Yue, J. C.; Luo, Z. Y. & Jiang, P. D. (2006a). Mechanically driven proton conduction in single δ-free F_oF_1-ATPase. *Biochem. Biophys. Res. Commun.* 347., 752-757

Liu, X. L; Zhang, Y.; Yue, J. C.; Jiang, P. D. & Zhang, Z. X. (2006b). F_oF_1-ATPase as biosensor to detect single virus. *Biochem. Biophys. Res. Commun.* 342., 1319-1322

Lo, P. K.; Metera, K. L. & Sleiman, H. F. (2010). Self-assembly of three-dimensional DNA nanostructures and potential biological applications. *Curr Opin Chem Biol*. 14., 597-607

Luo, T. J. M.; Soong, R.; Lan, E.; Dunn, B. & Montemagno, C. D. (2005). Photo-induced proton gradients and ATP biosynthesis produced by vesicles encapsulated in a silica matrix. *Nat. Mater*. 4., 220-224

Martin, G. L.; Heuvel, V. D. & Dekker, C. (2007). Motor proteins at work for nanotechnology. *Science*. 317., 333-336

Matsui, T. & Yoshida, M. (1995). Expression of the wild-type and the Cys-/Trp-less $\alpha_3\beta_3\gamma$ complex of thermophilic F_1-ATPase in *E. coli*. *Biochim. Biophys. Acta.* 1231., 139-146

Meier, T.; Morgner, N.; Matthies, D.; Pogoryelov, D.; Keis, S.; Cook, G. M.; Dimroth, P. & Brutschy, B. (2007). A tridecameric c ring of the adenosine triphosphate (ATP) synthase from the thermoalkaliphilic *Bacillus* sp. strain TA2.A1 facilitates ATP synthesis at low electrochemical proton potential. *Mol. Microbiol*. 65., 1181-192

Milgrom, Y. M. & Cross, R. L. (2005). Rapid hydrolysis of ATP by mitochondrial F_1-ATPase correlates with the filling of the second of three catalytic sites. *Proc. Natl. Acad. Sci. USA*. 102., 13831-13836

Mitome, N.; Suzuki, T.; Hayashi, S. & Yoshida, M. (2004). Thermophilic ATP synthase has a decamer c-ring: Indication of noninteger 10:3 H^+/ATP ratio and permissive elastic coupling. *Proc. Natl. Acad. Sci. USA*. 101., 12159-12164

Montemagno, C. & Bachand, G. (1999). Constructing nanomechanical devices powered by biomolecular motors. *Nanotechnology*. 10., 225-231

Moriyama, Y.; Iwamoto, A.; Hanada, H.; Maeda, M. & Futai, M. (1991). One-step purification of *E. coli* H^+-ATPase (F_1F_o) and its reconstitution into liposomes with neurotransmitter transporters. *J. Biol. Chem*. 266., 22141-22146

Muneyuki, E.; Makino, M.; Kamata, H.; Kagawa, Y.; Yoshida, M. & Hirata, H. (1993). Inhibitory effect of NaN_3 on the F_oF_1 ATPase of submitochondrial particles as related to nucleotide binding. *Biochim. Biophys. Acta*. 1144., 62-68

Nishizaka, T.; Oiwa,K.; Noji, H.; Kimura, S.; Muneyuki, E.; Yoshida, M. & Kinosita, K. (2004). Chemomechanical coupling in F_1-ATPase revealed by simultaneous observation of nucleotide kinetics and rotation. *Nat. Struct. Mol. Biol.* 11., 142-148

Noji, H.; Yasuda, R.; Yoshida, M.; Kinosita, K. Jr. (1997). Direct observation of the rotation of F_1-ATPase.*Nature*. 386., 299-302

Oster, G.; Wang, H. & Grabe, M. (2000). How F_o-ATPase generates rotary torque. *Phil. Trans. R. Soc. Lond. B*. 355., 523-528

Pänke, O. & Rumberg, B. (1996). Kinetic modelling of the proton translocating CF_oCF_1-ATP synthase from spinach. *FEBS Lett.* 383., 196-200

Pänke, O. & Rumberg, B. Kinetic modeling of rotary CF_oF_1-ATP synthase: storage of elastic energy during energy transduction. *Biochim. Biophys. Acta.* 1412., 118-128

Pogoryelov, D.; Yu, J. S.; Meier, T.; Vonck, J.; Dimroth, P. & Müller, D. J. (2005). The c_{15} ring of the Spirulina platensis F-ATP synthase: F_1/F_o symmetry mismatch is not obligatory. *EMBO rep*. 6., 1040-1044

Pogoryelov, D.; Krah, A.; Langer, J. D.;, Yildiz, Ö.; Faraldo-Góez, J. D. & Meier, T. (2010). Microscopic rotary mechanism of ion translocation in the F_o complex of ATP synthases. *Nat. Chem. Biol*. 6., 891-899

Rajagopal, K & Schneider, J. P. (2004). Self-assembling peptides and proteins for nanotechnological applications. *Curr Opin Struct Biol*. 14., 480-486

Ravshan, Z. S. & Yasunobu, O. (2004). Wide Nanoscopic Pore of Maxi-Anion Channel Suits its Function as an ATP-Conductive Pathway. *Biophys. J*. 87., 1672-1685

Rondelez, Y.; Tresset, G.; Nakashima, T.; Kato-Yamada, Y.; Fujita, H.; Takeuchi, S. & Noji, H. (2005). Highly coupled ATP synthesis by F_1-ATPase single molecules. *Nature*. 433., 773-777

Sakharov, D. V.; Nagelkerke, J. F. & Rijken, D. C. (1996). Rearrangements of the fibrin network and spatial distribution of fibrinolytic components during plasma clot lysis. *J. Biol. Chem.* 271., 2133-2138.

Saraste, M. (1999). Oxidative phosphorylation at the *fin desiécle*. *Science*. 283., 1488-1493

Seelert, H.; Poetsch, A.; Dencher, N. A.; Engel, A.; Stahlberg, H. & Müller, D. J. (2000). Structural biology: Proton-powered turbine of a plant motor. *Nature*. 405., 418-419

Senior, A. E.; Nadanaciva, S.; Weber, J. (2002). The molecular mechanism of ATP synthesis by F_1F_o-ATP synthase. *Biochim. Biophys. Acta*. 1553., 188-211

Sharma, V. K.; Teoh, H. T.; Wong, L. Y. H.; Su, J.; Ong, B. K. C. & Chan, B. P. L. (2010). Recanalization Therapies in Acute Ischemic Stroke: Pharmacological Agents, Devices, and Combinations. *Stroke Research and Treatment.* 2010., 672064

Shu, Y. G. & Shi, H. L. (2004). Cooperative effects on the kinetics of ATP hydrolysis in collective molecular motors. *Phys. Rev. E*. 69., 021912

Shu, Y. G. & Lai, P. Y. (2008). Systematic kinetics study of F_1F_o-ATPase: Analytic results and comparison with experiments. *J. Phys. Chem. B*. 112., 13453-13459

Shu, Y. G.; Yue, J. C. & Ou-Yang, Z. C. (2010). F_1F_o-ATPase, rotary motor and biosensor. *Nanoscale*. 2., 1284-1293

Soong, R. K.; Bachand, G. D.; Neves, H. P.; Olkhovets, A. G.; Craighead, H. G. & Montemagno, C. D. (2000).Powering an inorganic nanodevice with a biomolecular motor. *Science*. 290., 1555-1558

Steck, T. L.; Weinstein, R. S.; Straus, J. H.& Wallach, D. F. (1970). Inside-Out Red Cell Membrane Vesicles: Preparation and Puirification. *Science* 168.; 255-257

Steigmiller, S.; Turina, P. & Gräber, P. (2008). The thermodynamic H^+/ATP ratios of the H^+-ATP synthases from chloroplasts and *E. coli*. *Proc. Natl. Acad. Sci. USA*. 105., 3745-3750

Stock, D.; Leslie, A. G. W. & Walker, J. E. (1999). Molecular Architecture of the Rotary Motor in ATP Synthase. *Science.* 286., 1700-1705

Su, T.; Cui, Y. B.; Zhang, X. A.; Liu, X. L.; Yue, J. C.; Liu, N. & Jiang, P. D. (2006). Constructing a novel Nanodevice powered by δ-free F_1F_o-ATPase. *Biochem. Biophys. Res. Commun.* 350., 1013-1018

Sun, S. X.; Wang, H. & Oster, G. (2004). Asymmetry in the F_1-ATPase and its implications for the rotational cycle. *Biophys. J.* 86., 1373-1384

Tao, N.; Cheng, J. & Yue, J. C. (2008). Using F_1F_o-ATPase motors as micro-mixers accelerates thrombolysis. *Biochem. Biophys. Res. Commun.* 377., 191-194

Tao, N.; Cheng, J.; Wei, L. & Yue, J. C. (2009). Self-Assembly of F0F1-ATPase Motors and Ghost. *Langmuir*. 25., 5747-5752

Toei, M.; Gerle, C,; Nakano, M.; Tani, K,; Gyobu, N.; Tamakoshi, M.; Sone, N.; Yoshida, M.; Fujiyoshi, Y.; Mitsuoka, K. & Yokoyama, K. (2007). Dodecamer rotor ring defines H^+/ATP ratio for ATP synthesis of prokaryotic V-ATPase from *Thermus thermophilus*. *Proc. Natl. Acad. Sci. USA*. 104., 20256-20261

Turina, P.; Samoray, D. & Gräber, P. (2003). H^+/ATP ratio of proton transport-coupled ATP synthesis and hydrolysis catalysed by CF_oF_1-liposomes. *EMBO J.* 22., 418-426

Ueno, H.; Suzuki, T.; Kinosita, K. Jr. & Yoshida, M. (2005). ATP-driven stepwise rotation of F_oF_1-ATP synthase. *Proc. Natl. Acad. Sci. USA*. 102., 1333-1338

Wang, H. & Oster, G. (1998). Energy transduction in the F_1 motor of ATP synthase. *Nature*. 396., 279-282

Watanabe, R.; Iino, R. & Noji, H. (2010). Phosphate release in F_1-ATPase catalytic cycle follows ADP release. *Nat. Chem. Biol*. 6., 814-820

Weber, J. & Senior, A. E. (2003). ATP synthesis driven by proton transport in F_1F_o-ATP synthase. *FEBS Lett.* 545., 61-70

Weber, J. (2006). ATP synthase: Subunit-subunit interactions in the stator stalk. *Biochim. Biophys. Acta*. 1757., 1162-1170

Xing, J.; J. C. Liao, J. C. & Oster, G. (2005). Making ATP. *Proc. Natl. Acad. Sci. USA*. 102., 16539-16546

Yang, Q.; Liu, X. Y.; Miyake, J. & Toyotama, H. (1998). Self-assembly and immobilization of liposomes in fused-silica capillary by avidin-biotin binding. *Supramol. Sci*. 5., 769-772.

Yasuda, Y.; Noji, H.; Kinosita, K. Jr.; Yoshida, M. (1998). F_1-ATPase is a highly efficient molecular motor that rotates with discrete 120° steps. *Cell*. 93., 1117-1124

Yin, P.; Choi, H. M. T.; Calvert, C. R. & Pierce, N. A. (2008). Programming biomolecular self-assembly pathways. *Nature*. 451., 318-322

Zhang, Y. H.; Wang, J.; Cui, Y. B.; Yue, J. C. & Fang, X. H. (2005). Rotary torque produced by proton motive force in F_1F_o motor. *Biochem. Biophys. Res. Commun*. 331., 370-374

Zhang, Y.; Deng, Z. T.; Yue, J. C.; Tang, F. Q. & Wei, Q. (2007). Using cadmium telluride quantum dots as a proton flux sensor and applying to detect H9 avian influenza virus. *Anal. Biochem.* 364., 122-127

Zhao, X.; Pan, F.; Xu, H. Yaseen, M.; Shan, H.; Hauser, C. A.; Zhang, S.; Lu, J. R. (2010). Molecular self-assembly and applications of designer peptide amphiphiles. *Chem. Soc. Rev.* 39., 3480-98

Biomaterials Applications for Nanomedicine

Edited by Prof. Rosario Pignatello

ISBN 978-953-307-661-4
Hard cover, 458 pages
Publisher InTech
Published online 16, November, 2011
Published in print edition November, 2011

These contribution books collect reviews and original articles from eminent experts working in the interdisciplinary arena of biomaterial development and use. From their direct and recent experience, the readers can achieve a wide vision on the new and ongoing potentialities of different synthetic and engineered biomaterials. Contributions were selected not based on a direct market or clinical interest, but on results coming from a very fundamental studies. This too will allow to gain a more general view of what and how the various biomaterials can do and work for, along with the methodologies necessary to design, develop and characterize them, without the restrictions necessary imposed by industrial or profit concerns. Biomaterial constructs and supramolecular assemblies have been studied, for example, as drug and protein carriers, tissue scaffolds, or to manage the interactions between artificial devices and the body. In this volume of the biomaterial series have been gathered in particular reviews and papers focusing on the application of new and known macromolecular compounds to nanotechnology and nanomedicine, along with their chemical and mechanical engineering aimed to fit specific biomedical purposes.

How to reference

In order to correctly reference this scholarly work, feel free to copy and paste the following:

Jia-Chang Yue, Yao-Gen Shu, Pei-Rong Wang and Xu Zhang (2011). δ-Free FoF1-ATPase, Nanomachine and Biosensor, Biomaterials Applications for Nanomedicine, Prof. Rosario Pignatello (Ed.), ISBN: 978-953-307-661-4, InTech, Available from: http://www.intechopen.com/books/biomaterials-applications-for-nanomedicine/-free-fof1-atpase-nanomachine-and-biosensor

INTECH
open science | open minds

InTech Europe
University Campus STeP Ri
Slavka Krautzeka 83/A
51000 Rijeka, Croatia
Phone: +385 (51) 770 447
Fax: +385 (51) 686 166
www.intechopen.com

InTech China
Unit 405, Office Block, Hotel Equatorial Shanghai
No.65, Yan An Road (West), Shanghai, 200040, China
中国上海市延安西路65号上海国际贵都大饭店办公楼405单元
Phone: +86-21-62489820
Fax: +86-21-62489821

IntechOpen